To be submitted to Geophysical and Astrophysical Fluid Dynamics

Thermal Convection in a Rotating Shear Flow

David H. Hathaway
Space Science Laboratory
NASA Marshall Space Flight Center
Huntsville, AL 35812 USA

Richard C. J. Somerville
Scripps Institution of Oceanography
University of California, San Diego
La Jolla, CA 92093 USA

Abstract

A three-dimensional and time-dependent numerical model is used to simulate thermal convection imbedded in a shear flow in a rotating atmosphere. The fluid is confined to a plane parallel layer with periodic side boundaries, and the rotation vector is tilted from the vertical to represent a low-latitude region. An eastward mean flow is imposed which is constant with depth but has a jet-like profile in latitude. The convection is driven by a prescribed vertical temperature difference. Interactions between the shear flow and the convection extract energy from the mean flow and decrease the mean shear in the nonrotating case. In the presence of rotation, however, the convection can feed energy into the jet and enhance the mean shear. Mean meridional circulations are also produced by the effects of rotation. The Coriolis force on the vertical flows in these circulations contributes to the changes in the mean zonal wind. Three rotating cases are examined which show this behavior in varying degrees. A simple mechanism is described which explains how the convection can produce this countergradient flux of momentum in a

rotating layer. Although the system studied is highly idealized, it exhibits momentum fluxes and wave-like patterns which, for certain parameter values, are similar to those observed on Jupiter.

1. INTRODUCTION

Thermal convection plays a central role in generating many geophysical and astrophysical flows. In addition to its primary role of transporting heat, convection can also drive global circulations in rotating stars and planets. Although meridional circulations and differential rotation can be driven directly by thermal gradients, convection has also been shown to be an efficient driver of these flows [e.g. Gilman (1977), Busse (1982, 1983a), Hathaway and Somerville (1983) and references therein].

Gilman (1977), Glatzmaier (1984) and Gilman and Miller (1986) have shown by numerical simulation that the Sun's differential rotation is a natural consequence of the effects of rotation on convection in a thick rotating spherical shell of fluid. Weak meridional circulations are also produced in these simulations. Gilman and Miller (1986) have also shown that the shear in the differential rotation can feed back on the convection, altering the shape of the convective eddies so that a new balance is achieved in maintaining a stronger differential rotation. Hathaway and Somerville (1986) have examined additional examples of this positive feedback mechanism in numerical simulations of convection imbedded in a mean flow with a vertical shear. Nonlinear interations such as these, between convective eddies and mean flows, may also play an important role in driving the global circulations of Jupiter and Saturn.

Busse (1976) has suggested that large scale convection within Jupiter and Saturn may be responsible for the multiple jet streams seen in the differential rotation profiles of these

planets. Observationally, Beebe et al. (1980), Ingersoll et al. (1981) and Sromovsky et al. (1982) have found that the cloud motions in Jupiter's atmosphere indicate a transfer of energy and momentum from nonaxisymmetric eddies into the axisymmetric zonal winds. The nature of these eddies remains a subject of debate and thermal convection cannot be ruled out. Models for the internal structure of Jupiter and Saturn [Hubbard and Smoluchowski (1973), Graboski et al. (1975), Slattery (1977), DeCampli and Cameron (1979), and Hubbard and Horedt (1984)] indicate that the thermal stratification is superadiabatic throughout nearly all of their interiors. Recently, Ingersoll and Pollard (1982) and Busse (1983b) have shown in more detail how convection, in the form of columns aligned with the rotation axis, may drive the zonal jets on these planets.

Here we consider the possibility that nonlinear interactions between small scale thermal convection and a rotating shear flow might also be important for the dynamics of the atmospheres of Jupiter and Saturn. Our approach is to study a mechanism in isolation rather than attempting to include all the necessary physics required for a realistic simulation. The particular mechanism of interest is illustrated in Figure 1. We consider a sheared zonal wind in the form of an atmospheric jet stream and include convective motions imbedded in this flow. If the convection is distorted by the shear flow to form a chevron-like or herringbone pattern then the effects of rotation can produce a flux of momentum into the jet. Without rotation the convecting fluid flows directly from an updraft to a downdraft. In this

convective flow pattern the fluid moving toward the maximum of the jet carries westward momentum which converges on the jet and decreases the eastward flow. With rotation the convective flow is turned by the Coriolis force. This produces a component of the flow along the axes of the convective rolls. In this flow pattern the fluid moving toward the maximum of the jet carries eastward momentum which converges on the jet and increases the eastward flow. This simplified explanation presumes the existence of the jet as well as the production of a chevron-like convection pattern. It neglects any competing processes. While the relevance of this mechanism for Jupiter is uncertain, it does show quite simply how convection in the presence of rotation might feed momentum into a mean zonal flow.

The production of this chevron-like convection pattern requires an interaction between the convection and the shear flow which is similar in nature to the positive feedback mechanism described by Gilman and Miller (1986) and Hathaway and Somerville (1986). In order to determine whether such a pattern might be generated, and to see how the convective motions interact with the zonal wind, we numerically simulate the fully nonlinear convective motions in a rotating shear flow. The three-dimensional and time-dependent numerical model is described in the next section. The results of the calculations are described in the following section. The results illustrate the essential features of a process by which convection might influence the large-scale dynamics of rotating stars and planets.

2. THE MODEL

We have chosen an idealized system for this study. Although we use the full nonlinear equations for a fluid with both viscous and thermal diffusion, we assume that the fluid is Boussinesq, i.e. of constant density except for buoyancy effects due to temperature. We use a plane parallel layer of fluid which is positioned tangent to the planet at a latitude ϕ as shown in Figure 2. Although we neglect the effects of curvature, we include both the vertical and the horizonal components of the rotation vector. Our representation of the influence of rotation is quite general in that we have retained all of the Coriolis terms rather than making a priori assumptions concerning their relative magnitudes. We employ rigid (nonslip) top and bottom boundaries, and use periodic side boundaries to represent an infinite plane parallel layer. These periodic boundaries allow a wide range of convective patterns to form in the layer but preclude the use of curvature in the geometry. Again, we stress that our purpose here is to study a mechanism, not to simulate any actual atmospheric flow.

We impose an eastward zonal flow which is constant with depth but varies with latitude, the y direction, according to

$$U_o(y) = A \sin^2(\pi y/\lambda). \qquad (2.1)$$

Here λ is the latitudinal extent of the computational domain and A is the amplitude of the jet. This jet profile satisfies the mass continuity and thermal energy equations and makes the zonal

flow periodic so that it satisfies the horizontal boundary conditions. The top and bottom boundaries must also participate in this flow, so that (2.1) is satisfied on the boundaries as well as in the interior. If the boundaries were to remain at rest the basic state would have a vertical shear in addition to the horizontal shear. This added shear would complicate the physics and prevent us from examining this mechanism in isolation.

This jet profile is externally imposed and maintained. The source of the jet is not specified. It might be produced by the columnar convection described by Busse (1976, 1983), by baroclinic processes, by two-dimensional turbulent cascades or by mean meridional circulations. Our concern in this paper is with the interactions between the jet and thermally driven convective motions. Although the convection cannot alter the forcing mechanism for the jet, it can alter the jet itself by producing a mean zonal flow which may change the jet profile.

To be consistent, we must also include a mean pressure field, which depends upon both latitude and height, and the imposed force or Reynolds stress which maintains the imposed jet against viscous diffusion and the Coriolis force. The resulting balance can then be removed from the equations for the convection, thereby leaving the influence of the mean flow in the advective terms only.

We make the governing equations dimensionless by using D, the depth of the layer, as the unit of length, D^2/ν, the viscous diffusion time, as the unit of time and ΔT, the temperature

difference across the layer, as the unit of temperature. The dimensionless equations are then given by the mass continuity equation,

$$\frac{\partial u}{\partial x} + \frac{\partial v}{\partial y} + \frac{\partial w}{\partial z} = 0 \ , \tag{2.2}$$

the three components of the momentum equation.

$$\frac{\partial u}{\partial t} + [u+U_o] \frac{\partial u}{\partial x} + v\frac{\partial}{\partial y} [u+U_o] + w\frac{\partial u}{\partial z} - T_a^{1/2} \sin\phi v + T_a^{1/2} \cos\phi w$$

$$= - \frac{\partial p}{\partial x} + \nabla^2 u \tag{2.3}$$

$$\frac{\partial v}{\partial t} + [u+U_o] \frac{\partial v}{\partial x} + v\frac{\partial v}{\partial y} + w\frac{\partial v}{\partial z} + Ta^{1/2} \sin\phi u = - \frac{\partial p}{\partial y} + \nabla^2 v \tag{2.4}$$

$$\frac{\partial w}{\delta t} + [u+U_o] \frac{\partial w}{\partial x} + v\frac{\partial w}{\partial y} + w\frac{\partial w}{\partial z} - Ta^{1/2} \cos\phi u = - \frac{\partial p}{\partial z} + \frac{Ra}{Pr} T + \nabla^2 w \tag{2.5}$$

and the thermal energy equation,

$$\frac{\partial T}{\partial t} + [u+U_o] \frac{\partial T}{\partial x} + v\frac{\partial T}{\partial y} + w\frac{\partial}{\partial z} [T+T_o] = \frac{1}{Pr} \nabla^2 T \tag{2.6}$$

where

$$Ta = \frac{4\Omega^2 D^4}{\nu^2} \tag{2.7}$$

is the Taylor number,

$$Ra = \frac{\alpha g \Delta T D^3}{\kappa \nu} \tag{2.8}$$

is the Rayleigh number and

$$Pr = \frac{\nu}{\kappa} \tag{2.9}$$

is the Prandtl number. Here Ω is the rotation frequency, ν is the viscosity, κ is the thermal diffusivity, α is the volumetric coefficient of thermal expansion and g is the gravitational acceleration. The perturbed quantities include (u, v, w), the fluid velocity in the (x, y, z) direction, p, the pressure, and T, the temperature. The unperturbed temperature, in these dimensionless units, is given by

$$T_o(z) = 1 - z \ . \tag{2.10}$$

Equations (2.2) through (2.6) are solved numerically for the perturbed quantities subject to the boundary conditions that (u, v, w) and T vanish at the top and bottom boundaries and are periodic in x and y. The numerical procedure we use is an implicit finite difference technique suggested by Chorin (1968) and described in detail by Somerville and Gal-Chen (1979). The computational domain is one unit in the z (upward) direction by 10 units in the x (eastward) direction by 10 units in the y (northward) direction. The calculation involves 57,600 grid points in an array with 25 points in z, 48 points in x, and 48 points in y. One time step takes about 7 seconds on the CRAY1 machines at the National Center for Atmospheric Research.

3. THE ANALYSIS

Four simulations were run with the numerical code. All had $Ra = 10^4$, $Pr = 1.0$, $\phi = 20°$, and $A = 100$. The rotation rate was varied from one simulation to the next with $Ta = 0$, 1×10^4, 3×10^4, and 1×10^5. All four simulations were started from rest by introducing small random perturbations to the temperature field. These perturbations initiate convective motions which reach a statisticaly steady state after about 300 time steps. Each case was run for a total of 1000 time steps.

To determine the effect of the convection on the jet we average the x component of the momentum equation (equation 2.3) over x and z to find

$$\frac{\partial \langle u \rangle}{\partial t} + \frac{\partial \langle uv \rangle}{\partial y} + \langle v \rangle \frac{d}{dy} [\langle u \rangle + U_o] - Ta^{1/2} \sin\phi \langle v \rangle + Ta^{1/2} \cos\phi \langle w \rangle = \frac{\partial^2 \langle u \rangle}{\partial y^2} + \left\langle \frac{\partial^2 u}{\partial z^2} \right\rangle \qquad (3.1)$$

where

$$\langle a \rangle = \frac{1}{\lambda} \int_0^1 \int_0^\lambda a(x,y,z)\, dxdz \qquad (3.2)$$

represents an averaged quantity. From left to right in (3.1) we see that the average zonal flow, $\langle u \rangle$, induced by the convective motions is influenced by the divergence of the momentum flux $\langle uv \rangle$, the latitudinal advection of the mean zonal flow, the Coriolis force on a mean meridional flow, the Coriolis force on a mean vertical flow and viscous diffusion. The mean zonal velocity is given by

$$U = U_o + \langle u \rangle \ . \tag{3.3}$$

The mean kinetic energy in the zonal wind is given by

$$\overline{KE_x} = \frac{1}{\lambda} \int_0^{\lambda} \frac{1}{2} U^2 \, dy \ . \tag{3.4}$$

We can determine the balance that maintains this kinetic energy by considering its time derivative and using (3.1) with an integration by parts. We find

$$\frac{\partial \overline{KE}_x}{\partial t} = \frac{1}{\lambda} \int_0^{\lambda} \left[\langle uv \rangle \frac{dU}{dy} + Ta^{1/2} \sin\phi \langle v \rangle U - Ta^{1/2} \cos\phi \langle w \rangle U \right] dy + \tag{3.5}$$

$$+ \frac{1}{\lambda} \int_0^{\lambda} \left[U \frac{d^2 \langle u \rangle}{dy^2} + U \left\langle \frac{\partial^2 u}{\partial z^2} \right\rangle \right] dy \ .$$

For a steady state a balance is maintained between the source terms (the first integral on the right hand side) and viscous diffusion (the second integral on the right hand side). The source terms include, from left to right, a countergradient flux of momentum by the convective motions, a transfer of energy from the y kinetic energy component by the Coriolis force, and a transfer of energy from the z kinetic energy component by the Coriolis force. The important source term is the first one since this represents a net source of mean kinetic energy from the fluctuating part of the flow rather than a transfer between different components of the mean kinetic energy. Thus, a

positive correlation between the momentum flux <uv> and the mean zonal wind gradient, $\frac{dU}{dy}$, indicates that the convective motions are feeding energy into the mean zonal flow.

Our analysis of the four simulations includes determining the structure of the convective velocity and temperature fields for each case together with calculations of the mean momentum and energy balance.

3a. Ta = 0

Figure 3 shows a three-dimensional perspective view of the velocity and temperature fields for the final time step of the nonrotating case (Ta = 0). Color is used to represent temperature with yellow being hot and red being cold. The velocity field is indicated by the trajectories of 700 markers that are constrained to move along the three visible surfaces. Although a chevron pattern is not produced by the convection in this case, the effects of the shear flow are still quite evident. The maximum in the imposed zonal flow occurs midway between the northern and southern boundaries of the computational domain illustrated in Figure 3. On either side of the maximum, where the latitudinal shear is strongest, the convection forms elongated cells which are aligned east-west with the mean flow. The trajectories plotted on the upper surface show outflows from the hot updrafts and inflows along the downdrafts. Typical dimensionless velocities associated with the convective motions are about 19 for this case and the heat flux is 2.45 times that carried by thermal conduction alone.

Figure 4 shows the averaged quantities for this nonrotating case. In addition to averaging over x and z we have also averaged over a time period covering the last half of the simulation in obtaining these quantities. The left hand panel shows the imposed zonal flow as a dotted line and the total zonal flow in the presence of convection as a solid line. The decrease in the maximum velocity from 100 to 96 and the increase in the minimum from 0 to 2 shows quite readily that energy and momentum are being extracted from the imposed zonal flow. This conclusion is supported by the analysis shown in the right hand panel of Figure 4. Here the shear, $\partial U/\delta y$, is plotted as a solid line and the momentum flux, $\langle uv \rangle$, is plotted as a dashed line. The strong anticorrelation between these two quantities is further evidence that energy is extracted from the mean zonal wind by a down-gradient flux of zonal momentum. Integrating the product of these two quantities over y gives a net rate of loss of zonal kinetic energy of -923 while the mean zonal kinetic energy level is 1875.

3b. $Ta = 1 \times 10^4$

Figure 5 shows the temperature and velocity fields for the rotating case with $Ta = 1 \times 10^4$. Although a chevron pattern is not well formed there is some suggestion of one. Where the shear is strong the convective rolls tend to be angled in the same sense as illustrated in Figure 1, especially on the northern edge of the jet. The fluid motions show some turning by the Coriolis force but substantial flows parallel to the axes of the

convective rolls are not obvious. Typical convective velocities are about 15 and the heat flux is reduced to 1.95 times the conductive heat flux.

Figure 6 shows the averaged quantities for this rotating case. The mean zonal flow is nearly equal to the imposed zonal flow except near the jet minima where the mean flow becomes a weak westward flow. The mean shear and the momentum flux plotted in the right hand panel do not appear to be well correlated. However, the integral of their product gives a small net rate of gain of zonal kinetic energy of +48 for a mean zonal kinetic energy of 1875.

For this rotating case we must also consider the Coriolis terms in the balance equations (3.1) and (3.5). The Coriolis force acting on a mean meridional flow or a mean vertical flow can also alter the momentum and energy in the mean zonal wind. We find that the mean meridional flow, $\langle v \rangle$, is extremely small. Although weak meridional circulations are induced, they have oppositely directed flows in the upper and lower halfs of the layer which cancel to give $\langle v \rangle \approx 0$. There is, however, a mean vertical flow, $\langle w \rangle$, associated with these induced circulations. Thus, in equation (3.1) for the mean zonal momentum the two important terms are the momentum flux divergence, $\partial \langle uv \rangle / \partial y$, and the Coriolis force, $Ta^{1/2} \cos\phi \langle w \rangle$, on the mean vertical flow. These two quantities are plotted as functions of y in Figure 7. For this case these mean quantities appear to be noisy and insignificant with the exception of mean vertical flows near the jet minima with rising motions on the southern edge and sinking

motions to the north. These mean vertical flows tend to produce a westward flow near the southern edge and an eastward flow to the north as is seen in the mean zonal flow plotted in Figure 6. The net rate of loss of mean zonal kinetic energy due to this Coriolis term is -67.

3c. $Ta = 3 \times 10^4$

Figure 8 shows the velocity and temperature fields for the moderately rotating case with $Ta = 3 \times 10^4$. Here a chevron pattern is fairly well established. The convection forms a herringbone pattern around the jet maximum with slanted rolls in the regions of strong shear on either side. A motion picture was produced of the time evolution of the convection. It shows the wavelike cells in the jet maximum propagating eastward at about the flow speed of the jet maximum. The slanted convection rolls on either side of the maximum are continually sheared by the flow and repeatedly detached and then reconnected with the waves in the jet maximum. The flow within these convective elements is turned by the Coriolis force to produce substantial flows along the axes of these features. The typical convective velocities in this case are about 11 and the dimensionless heat flux is 1.60.

The averaged quantities for this case are shown in Figure 9. There is a stronger eastward flow just to the north of the jet maximum and a westward flow is produced at the minimum. There appears to be a fairly strong positive correlation between the momentum flux and the velocity gradient as shown in the right hand panel. The integral of the product of these two quantities

gives a net rate of gain of mean zonal kinetic energy of +259. This result indicates that energy and momentum are being fed into the mean zonal wind by this counter gradient flux of zonal momentum.

In this case, as in the previous one, the mean meridional flow, $\langle v \rangle$, is insignificant, but the mean vertical flow plays a substantial role. The momentum flux divergence and the Coriolis term are plotted for comparison in Figure 10. Both are significant, but they tend to be opposed to one another. The Coriolis term appears to dominate, although weakly, in several places. The Coriolis term appears to be largely responsible for the westward flow in the jet minimum where the momentum flux divergence vanishes. The eastward flow on the northern edge of the jet maximum can be attributed to a positive correlation between the two driving terms at that location. For the mean kinetic energy, this Coriolis term gives a net rate of gain of kinetic energy of +113.

3d. $Ta = 1 \times 10^5$

The velocity and temperature fields for the rapidly rotating case with $Ta = 1 \times 10^5$ are shown in Figure 11. In this case, a new phenomenon appears. The convection is confined to the region of the jet maximum. This effect can be attributed to the tilted rotation vector. Hathaway and Somerville (1983) showed that the tilted rotation vector favors convection in the form of rolls aligned north-south, parallel to the horizontal component of the rotation vector. The previous cases indicate that the horizontal

shear on either side of the jet maximum favors convection in the form of rolls aligned with the shear. We propose that for this rapidly rotating case the convection is stabilized in these regions by the competition between the shear flow and the tilted rotation vector for opposing roll orientation (Hathaway and Somerville; 1985, 1986). The stabilizing effect of rotation is also evident in the slower convective velocities of 6 and the weaker heat flux (1.19 in dimensionless units).

The averaged quantities for this case are plotted in Figure 12. The mean zonal flow exhibits an increase in the eastward flow on the northern edge of the jet maximum and little change from the imposed flow elsewhere. The right hand panel shows that there is a positive correlation between the momentum flux and the velocity gradient. The integral of the product of these two quantities gives a rate of gain of kinetic energy of +68. This is much smaller than in the previous case as might be expected from the weakened convection.

Figure 13 shows the momentum flux divergence and the Coriolis term for this case. Again, these quantities are anticorrelated and the Coriolis term appears to be slightly stronger. The eastward flow that is induced on the northern edge of the jet maximum is the product of a local positive correlation between these two sources of zonal momentum. In spite of the apparent strength of this Coriolis term in the momentum balance, we find that it plays a lesser role in the kinetic energy balance. The rate of loss of mean zonal kinetic energy due to this term is -9.

The results of the analysis for these four simulations are summarized in Table 1. The top line indicates the Taylor number or rotation rate for each of the cases studied. The second line gives the magnitude of the convective velocities for each case. The third line gives the dimensionless heat flux (Nusselt number). The fourth line gives the rate of gain or loss of mean zonal kinetic energy due to the convective momentum flux and the last line gives the rate of change of mean zonal kinetic energy due to the Coriolis force on the induced mean vertical motions.

Several trends can be seen in this data. The convective velocities and the heat flux are diminished as the rotation rate is increased from one case to the next across Table 1. This illustrates the stabilizing effect of rotation on the convection (e.g. Hathaway and Somerville, 1983). The convective momentum flux gives a rapid loss of mean zonal kinetic energy for Ta = 0 but gives increasingly larger gain rates for Ta = 1×10^4 and Ta = 3×10^4. The rate of gain decreases for Ta = 1×10^5 primarily because of the weaker convection for that case.

A systemmatic trend is not evident in the rate of change of mean zonal kinetic energy due to the Coriolis force on the mean vertical flow. For Ta = 1×10^4 it gives a rate of loss of kinetic energy that is slightly greater than the rate of gain due to the momentum flux. For Ta = 3×10^4 it becomes a source of kinetic energy that augments the gain due to the momentum flux. For Ta = 1×10^5 it gives a loss again, albeit a small loss compared to the gain by the momentum flux.

4. CONCLUSIONS

We have used a three-dimensional and time-dependent numerical model to simulate convection in the presence of a jet-like zonal flow. We find that rotation plays a vital role in the dynamics. Without rotation the convective motions extract energy and momentum from the mean zonal flow. With rotation the convective motions feed energy and momentum into the mean flow.

Anisotropy in the convection is an instrumental part of this interaction between the perturbations and the mean flow. The shape of the convection cells is influenced by both the zonal flow and the tilted rotation vector. Hathaway and Somerville (1983) showed that the tilted rotation vector favors convection in the form of rolls oriented north-south, parallel to the rotation axis. Here we find that in the absence of rotation the horizontal shear in the zonal flow favors convection in the form of rolls oriented east-west, parallel to the zonal flow. For the first two rotating cases, with $Ta = 1 \times 10^4$ and $Ta = 3 \times 10^4$, these two processes produce convection in the form of a chevron or herringbone pattern. For the rapidly rotating case, with $Ta = 1 \times 10^5$, the competition between these two processes tends to stabilize the convection where the shear is strong, leaving north-south oriented convective rolls where the shear vanishes.

The fluid flows within these anisotropic convective patterns drive large scale circulations. As described by Hathaway and Somerville (1983), a mean flow with vertical shear is produced in the presence of the tilted rotation vector alone. This flow is directed to the southeast along the bottom of the layer and to

the northwest along the top. Since the vertical average of this flow is zero it does not contribute to the dynamics of the zonal jet. However, superimposed on this flow is a series of meridional circulations with rising motions on the southern edges of the jet maximum and minimum and sinking motions on the northern edges. The Coriolis force on these induced mean vertical motions is important for the zonal jet. Eastward flows are produced in the downdrafts and westward flows are produced in the updrafts.

The convective motions can also feed energy and momentum directly into the mean zonal flow by the mechanism illustrated in Figure 1. The Coriolis force turns the convective flow to introduce a velocity component along the axes of the convective rolls. If the convection forms a herringbone pattern, this gives a counter-gradient flux of momentum which enhances the mean zonal flow. The combined effects of rotation and the shear flow itself conspire to produce this herringbone pattern. The shear flow favors convective rolls aligned with the shear while rotation favors convective rolls aligned with the tilted rotation vector. When both of these effects are of similar magnitude the convective rolls are tilted from a north-south orientation and angle into the jet streams to produce the herringbone pattern and the counter-gradient flux of zonal momentum.

This effect may be evident in the cloud motions in Jupiter's atmosphere (Beebe et al., 1980; Ingersoll et al., 1981; Sromovsky et al., 1982). A distinct chevron pattern is visible in the clouds surrounding the prominent eastward jet at about 23° north

latitude as shown in Figure 14. The analyses of the cloud motions in this region indicate the presence of a counter-gradient flux of momentum. Although the source and nature of these cloud motions is uncertain, thermal convection and the effects seen in these simulations may play an important role.

The convective patterns and the dynamical properties of the flows produced in these idealized simulations are further evidence that convection can do much more than simply transport heat in stars and planets. The effects of rotation and the interactions between convection and large scale mean flows can have important consequences for the global circulation patterns of these astrophysical objects.

ACKNOWLEDGEMENTS

One of us (Hathaway) was employed by the National Solar Observatory of the National Optical Astronomy Observatories (NOAO) during much of this work. NOAO is operated by the Associaton of Universities for Research in Astronomy, Inc., under contract AST 78-17292 with the National Science Foundation. We are grateful for their support of this project. The calculations described in this paper were done on the CRAY computers at the National Center for Atmospheric Research (NCAR). We wish to thank NCAR and its Scientific Computing Division for their grant of this machine time. The research was also supported in part by the California Space Institute of the University of California.

REFERENCES

Beebe, R. F., Ingersoll, A. P., Hunt, G. E., Michell, J. L., and Mueller, J. P., "Measurements of wind vectors, eddy momentum transports, and energy conversions in Jupiter's atmosphere from Voyager 1 images," Geophys. Res. Lett. 7, 1-4 (1980).

Busse, F. H., "A simple model of convection in the Jovian atmosphere," Icarus 29, 255-260 (1976).

Busse, F. H., "Thermal convection in rotating systems," Proc. 9th U.S. Nat. Cong. Appl. Mech., Amer. Soc. Mech. Eng., New York, 299-305 (1982).

Busse, F. H., "Generation of mean flows by the thermal convection," Physics 9D, 287-299 (1983a).

Busse, F. H., "A model of mean zonal flows in the major planets," Geophys. Astrophys. Fluid Dynamics 23, 153-174 (1983b).

Chorin, A. J., "Numerical solutions of the Navier-Stokes equations," Math. Comput. 22, 743--762 (1968).

DeCampli, W. M. and Cameron, A.G.W., "Structure and evolution of isolated giant gaseous protoplanets," Icarus 38, 367-391 (1979).

Gilman, P. A., "Nonlinear dynamics of Boussinesq convection in a deep rotating spherical shell-I", Geophys. Astrophys. Fluid Dynam. 8, 93-135 (1977).

Gilman, P. A. and Miller, J., "Nonlinear convection of a compressible fluid in a rotating spherical shell", Astrophys. J. Suppl. in press (1986).

Glatzmaier, G. A., "Numerical simulations of stellar convective dynamos. I. The model and the method", J. Comp. Phys. 55, 461-484.

Graboske, H. C., Pollack, J. B., Grossman, A. S., and Olness, R. J., "The structure and evolution of Jupiter: The fluid contraction stage," Astrophys. J. 199, 265-281 (1975).

Hathaway, D. H. and Somerville, R.C.J., "Three-dimensional simulations of convection in layers with tilted rotation vectors," J. Fluid Mech. 126, 75-89 (1983).

Hathaway, D. H. and Somerville, R.C.J., "Numerical simulations in three space dimensions of time-dependent thermal convection in a rotating fluid," Lect. Appl. Math. 22, 309-319 (1985).

Hathaway, D. H. and Somerville, R.C.J., "Nonlinear interactions between convection, rotation, and flows with vertical shear," J. Fluid Mech. 164, 91-105 (1986).

Hubbard, W. B. and Smoluchowski, R., "Structure of Jupiter and Saturn," Space Sci. Rev. 14, 599-662 (1973).

Hubbard, W. B. and Horedt, G. P., "Computation of Jupiter's interior models from gravitational inversion theory," Icarus 54, 456-465 (1983).

Ingersoll, A. P., Beebe, R. F., Mitchell, J. L., Garneau, G. W., Yagi, G. M., and Mueller, J. P., "Interactions of eddies and mean zonal flow on Jupiter as inferred from Voyager 1 and Voyager 2 images," J. Geophys. Res. 86, 8733-8743 (1981).

Ingersoll, A. P. and Pollard, D., "Motion in the interiors and atmospheres of Jupiter and Saturn: Scale analysis, anelastic equations, barotropic stability criterion," Icarus 52, 62-80 (1982).

Slattery, W. L., "The structure of the planets Jupiter and Saturn," Icarus 32, 58-72 (1977).

Somerville, R.C.J. and Gal-Chen, T., "Numerical simulation of convection with mean vertical motion," J. Atmos. Sci. 36, 805-815 (1979).

Sromovsky, L. A., Revercomb, H. E., Suomi, V. E., Limaye, S. S., and Krauss, R. J., "Jovian winds from Voyager 2. Part II: Analysis of eddy transports," J. Atmos. Sci. 39, 1433-1445 (1982).

FIGURE CAPTIONS

Figure 1. Schematic illustration showing how convection might interact with a jet-like mean flow. Part a shows convection in a chevron or herringbone pattern in the absence of rotation. The convective motions carry fluid directly from warm updrafts to cold downdrafts. Momentum is extracted from the mean flow by these motions. Part b shows the effect of rotation on the convective motions. The Coriolis force turns the fluid flow along the axes of the convective rolls. Here momentum is fed into the mean flow.

Figure 2. The geometry and orientation of the computational domain. The plane-parallel layer is positioned tangent to the spherical shell at a latitude ϕ so that the rotation vector is tilted from the vertical. The x-direction is eastward, the y-direction is northward, and the z-direction is upward.

Figure 3. The velocity and temperature fields for the nonrotating case, Ta = 0. Temperature is represented by color with yellow being hot and red being cold. The convective velocity field is illustrated by the trajectories of small markers. The imposed flow is constant with depth and vanishes at the southern and northern boundaries. It has its maximum eastward velocity midway between these two boundaries. On either side of the jet maximum the convection forms rolls which tend to be aligned with the shear flow.

Figure 4. The mean quantities for the case with Ta = 0. The imposed zonal flow is represented by the dotted line in the left hand panel. The mean zonal flow in the presence of convection is represented by the solid line. The mean flow is noticeably weaker than the imposed flow. The right hand panel shows the momentum flux $\langle uv \rangle$ as a dashed line and the gradient of the mean flow as a solid line. The anticorrelation of these two quantities indicate that momentum and energy are extracted from the imposed flow by a downgradient flux of momentum in the convection.

Figure 5. The velocity and temperature fields for the rotating case with $Ta = 1 \times 10^4$. The convective rolls are narrower than in the nonrotating case and show a tendency to be slanted in the direction of the shear.

Figure 6. The mean quantities for the rotating case with $Ta = 1 \times 10^4$. The left hand panel shows that the mean flow is only slightly changed from the imposed flow. The right hand panel shows a weak correlation between the momentum flux and the gradient of the mean flow which suggests a countergradient flux of momentum is produced by the effects of rotation on the convection.

Figure 7. A comparison of the momentum flux divergence, dotted, line, and the Coriolis force on the induced mean vertical flow for the case with Ta = 1 x 10^4. Both terms are fairly weak and noisy except for the Coriolis force on the mean vertical motions around the jet minimum.

Figure 8. The velocity and temperature fields for the rotating case with Ta = 3 x 10^4. The convection forms a fairly distinct chevron or herringbone pattern. The Coriolis force turns the convective flow to produce substantial flows along the axes of these features. This produces a flux of momentum into the mean flow.

Figure 9. The mean quantities for the rotating case with Ta = 3 x 10^4. The mean flow is definitely stronger than the imposed flow. The momentum flux is well correlated with the gradient of the mean flow. This indicates that a countergradient flux of momentum is produced by the effects of rotation on the convection.

Figure 10. A comparison of the momentum flux divergence and the Coriolis force on the mean vertical flow. Both terms are substantial and tend to be opposed to each other.

Figure 11. The velocity and temperature fields for the rapidly rotating case with Ta = 1 x 10^5. The convection is concentrated in the vicinity of the jet maximum and forms a series of cells that are elongated in the north-south direction.

Figure 12. The mean quantities for the rapidly rotating case with Ta = 1 x 10^5. The mean zonal flow is enhanced in the vicinity of the jet maximum but is nearly equal to the imposed flow elsewhere. The momentum flux and the gradient of the mean zonal flow are correlated but the flux is not as strong as in the more slowly rotating case.

Figure 13. A comparison of the momentum flux divergence and the Coriolis force on the mean vertical flow. Both sources of zonal momentum are strong but they tend to be opposed to each other.

Figure 14. A chevron-like cloud pattern seen in Jupiter's north temperature belt by Voyager 2. The north temperature current runs east-west through the center of this region with wind speeds near 130 m/s.

Table 1

Ta	0	1×10^4	3×10^4	1×10^5
$\left[\int_0^1 (\langle u^2\rangle + \langle v^2\rangle + \langle w^2\rangle)dz\right]^{1/2}$	19	15	11	6
$\left[1 + \int_0^1 \langle wT\rangle dz\right]$	2.45	1.95	1.60	1.19
$\left[\frac{1}{\lambda}\int_0^\lambda \langle uv\rangle \frac{dU}{dy}\, dy\right]$	-923	+48	+259	+68
$-\left[\frac{1}{\lambda}\int_0^\lambda Ta^{1/2}\cos\phi \langle w\rangle U dy\right]$	0	-67	+113	-9

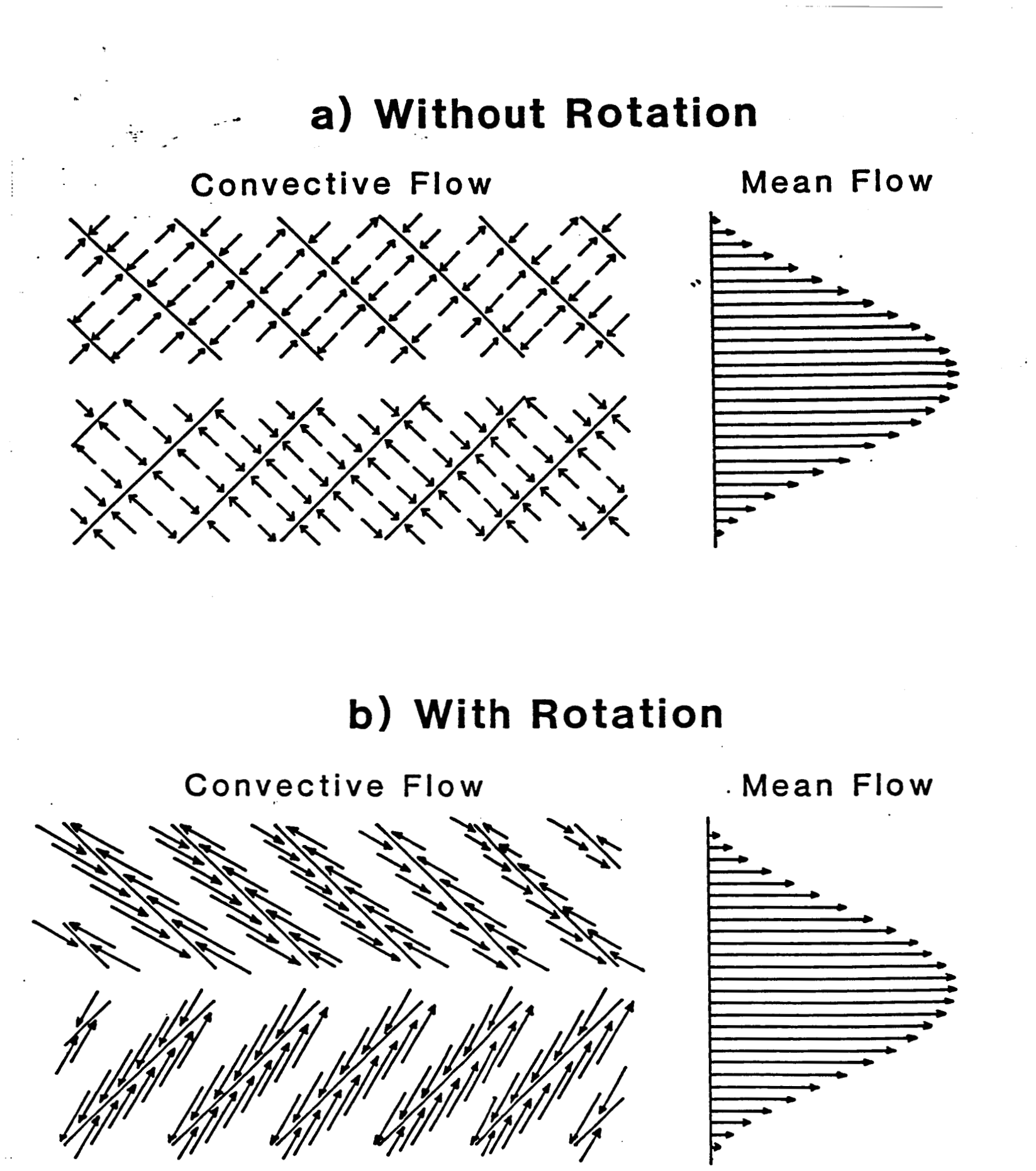
a) Without Rotation
Convective Flow
Mean Flow
b) With Rotation
Convective Flow
Mean Flow

Figure 1

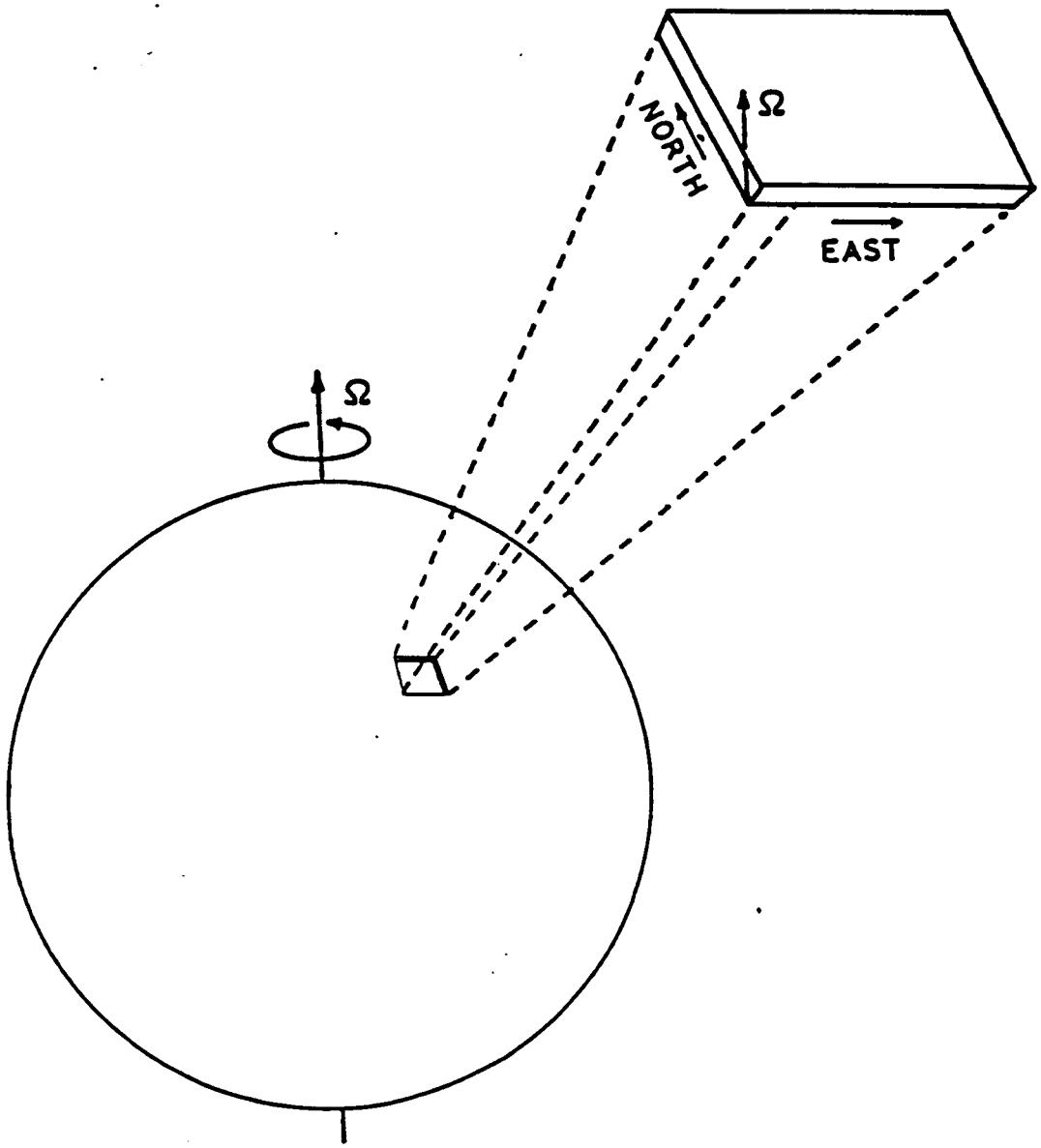

Figure 2

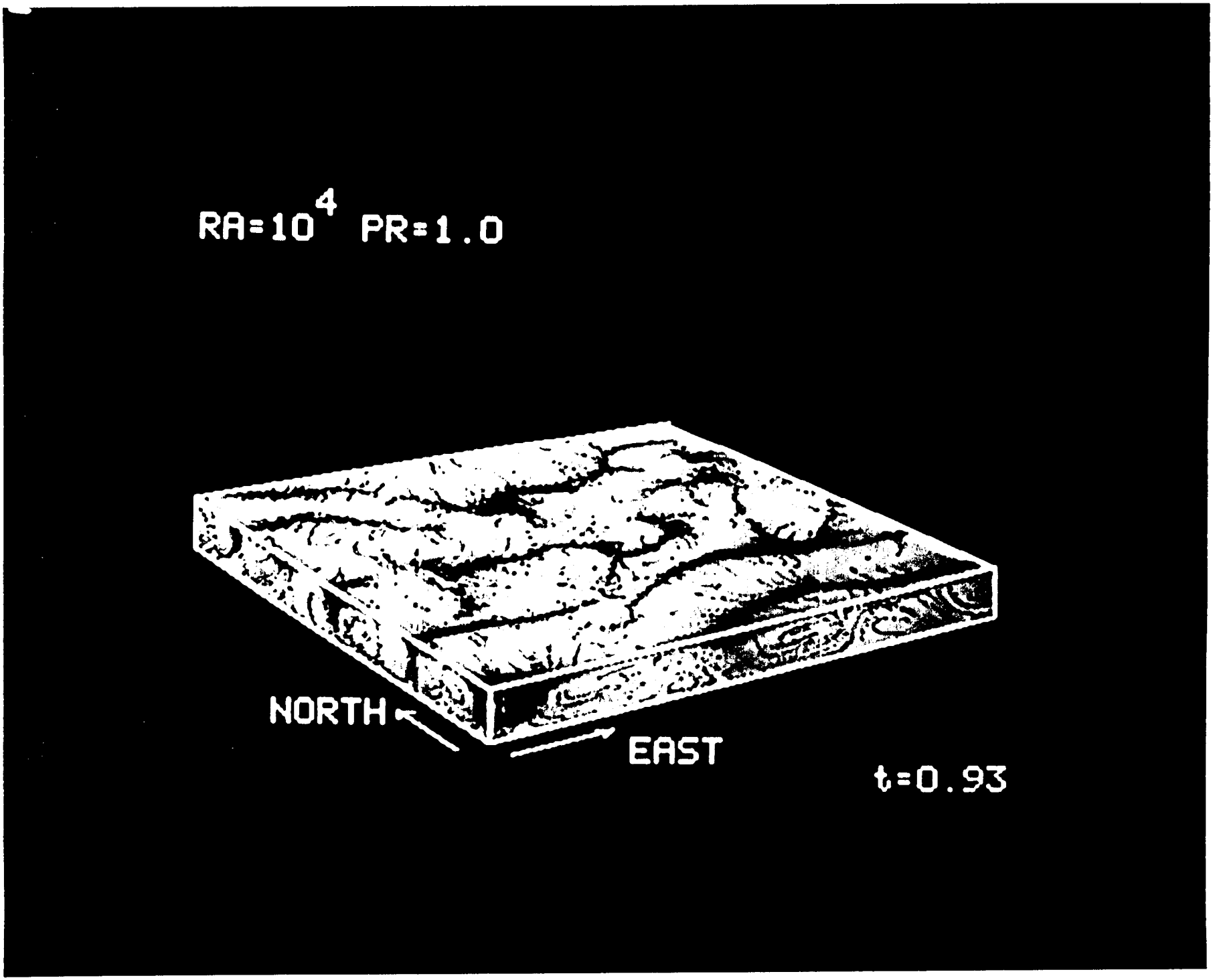
RA=10^4 PR=1.0
NORTH
EAST
t=0.93

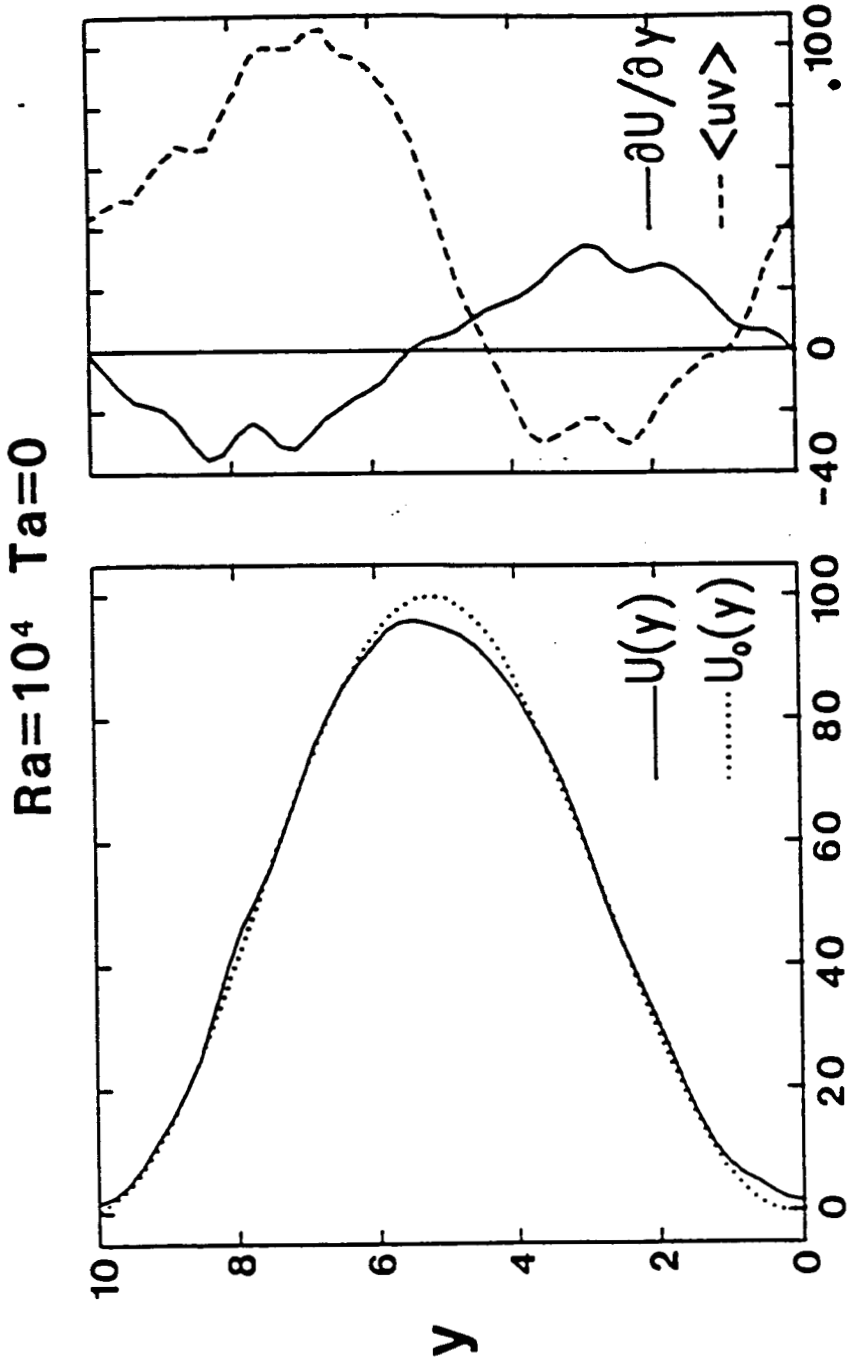

Figure 4

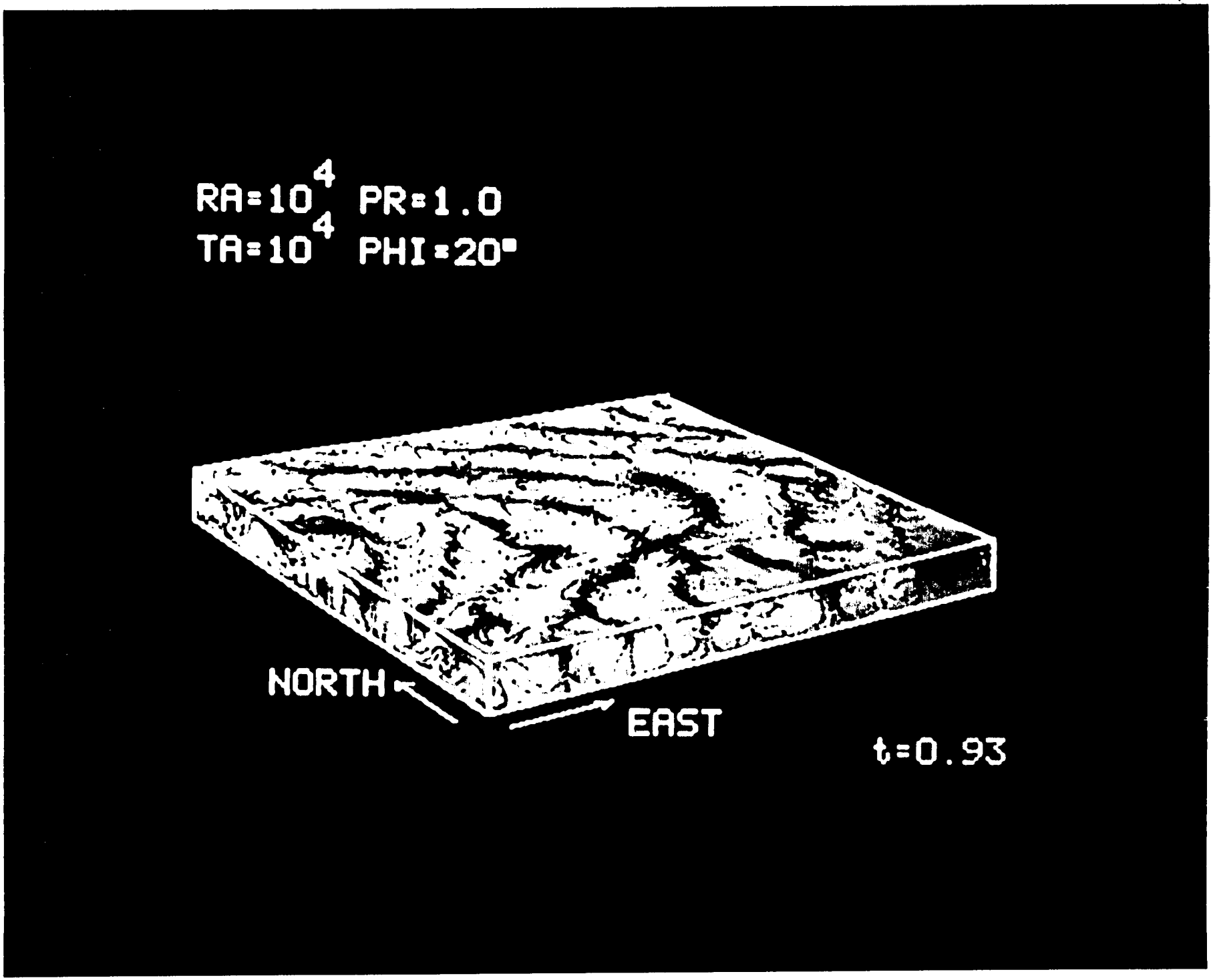
RA=10^4 PR=1.0
TA=10^4 PHI=20°
NORTH
EAST
t=0.93

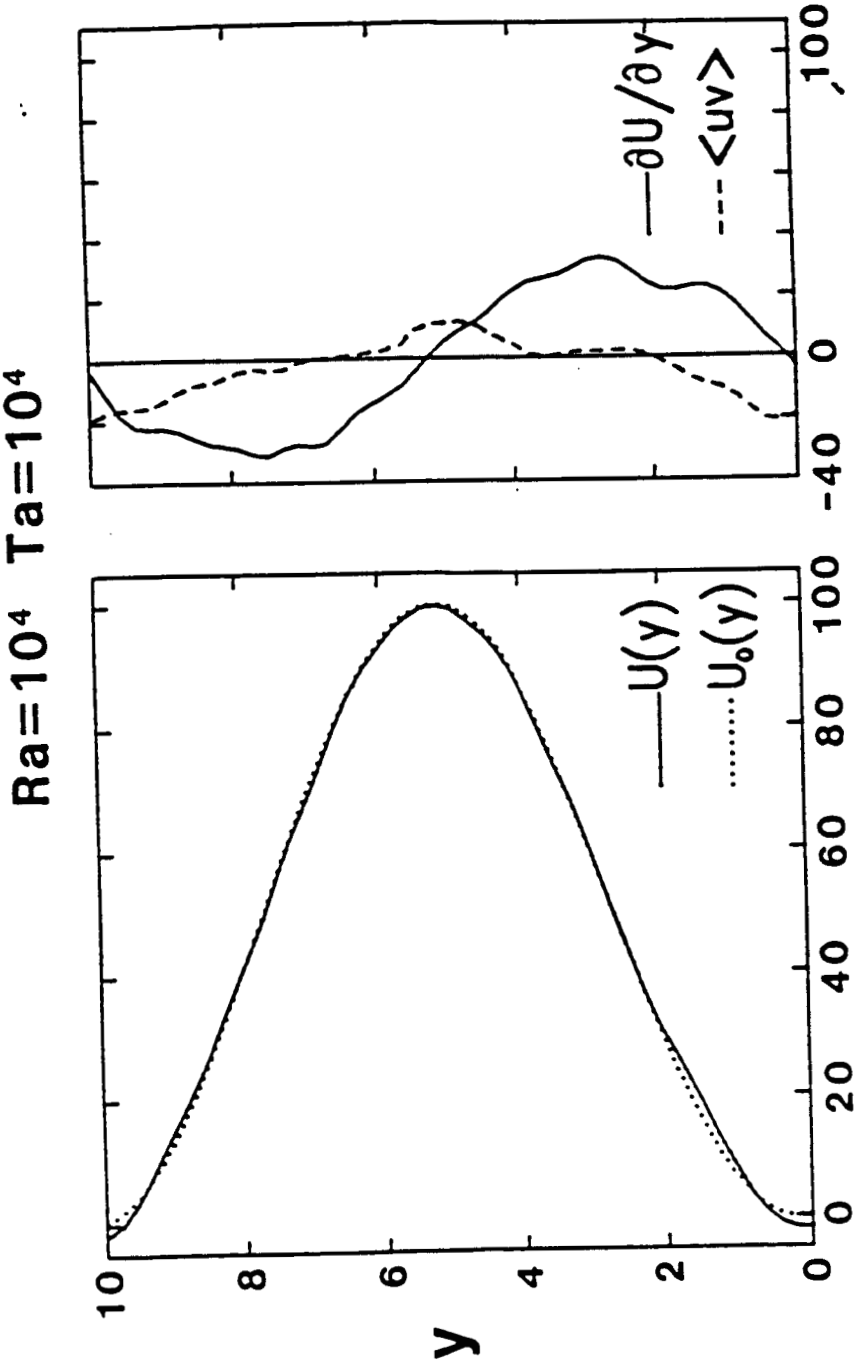

Figure 6

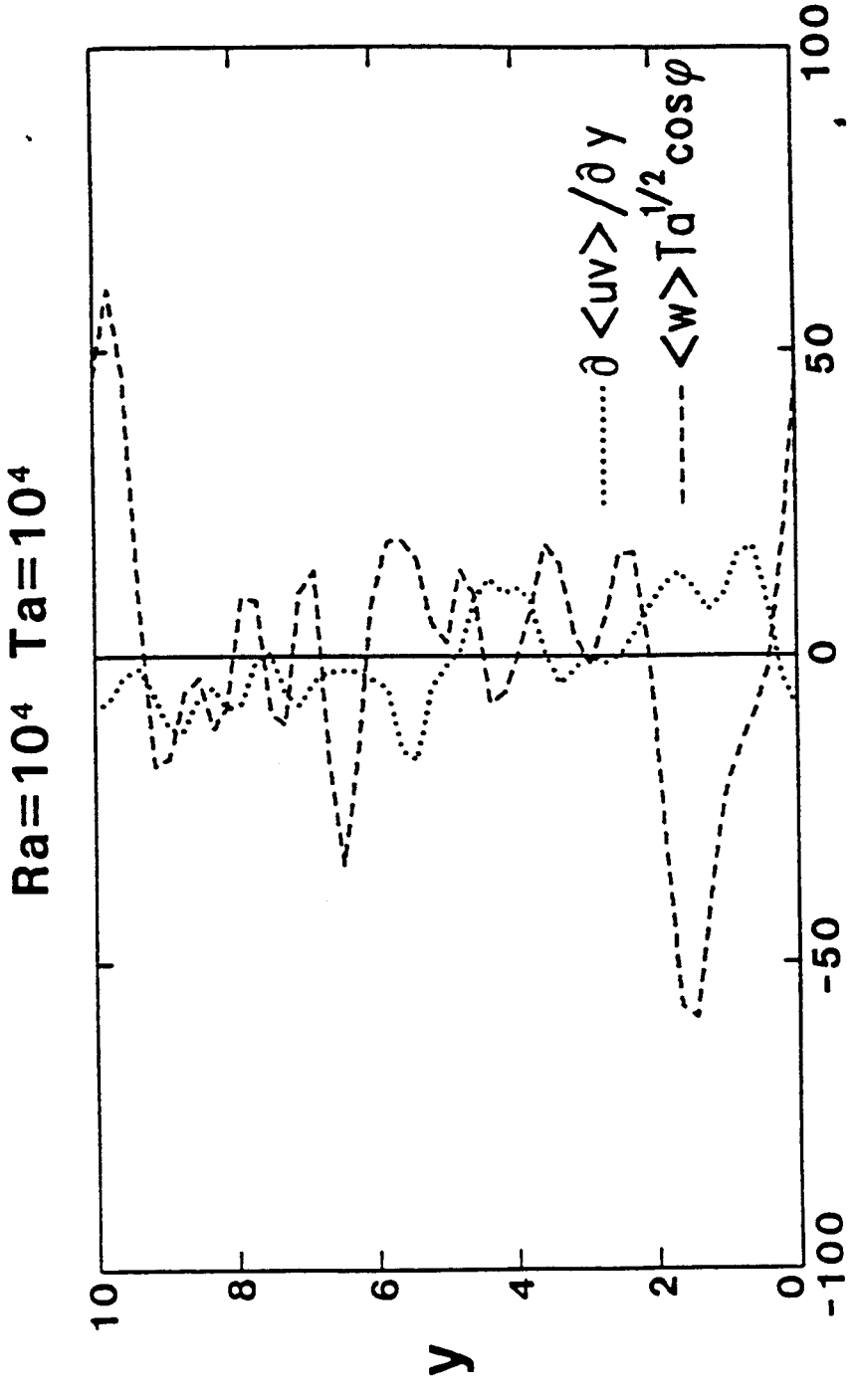

Figure 7

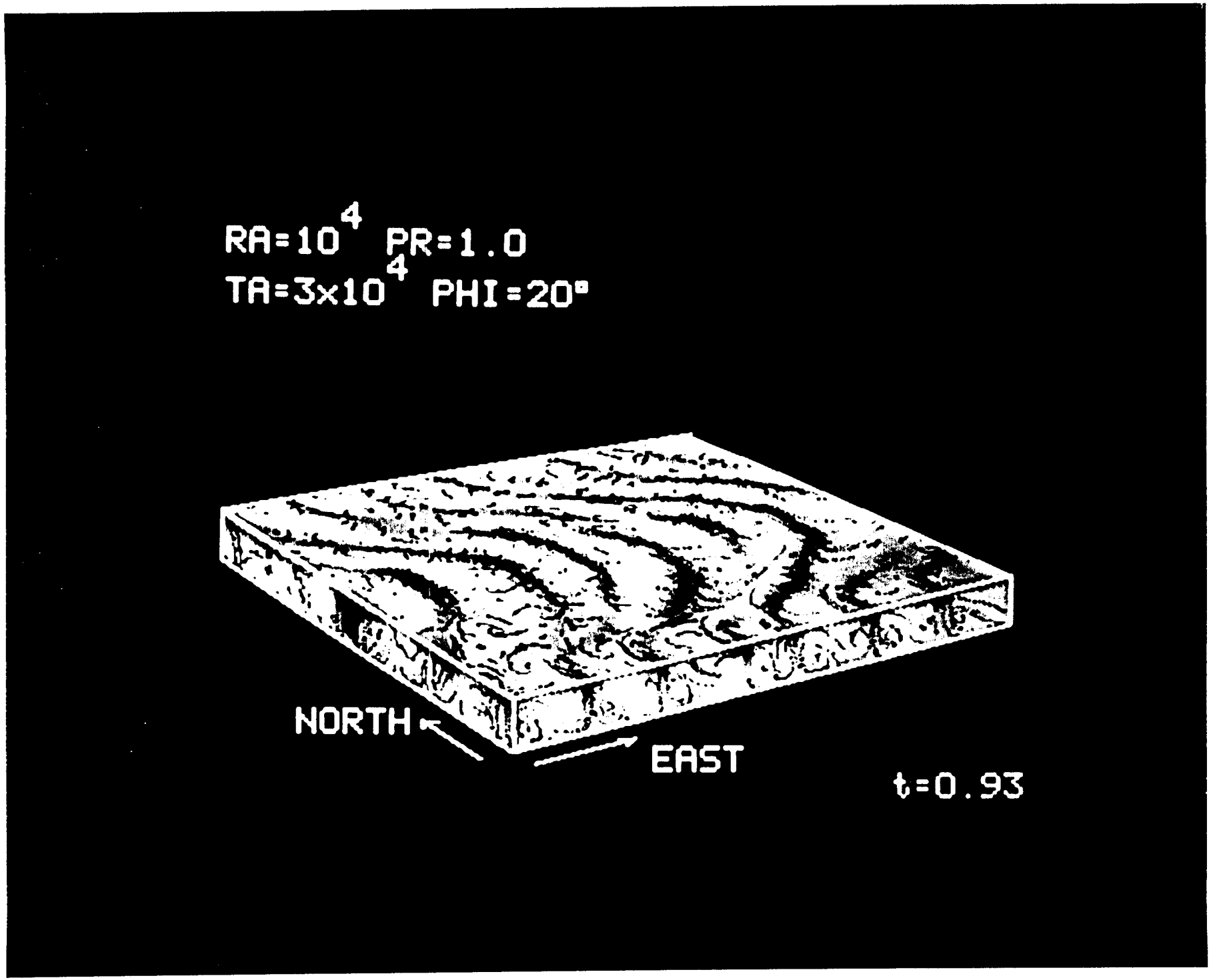
RA=10^4 PR=1.0
TA=3x10^4 PHI=20°
NORTH
EAST
t=0.93

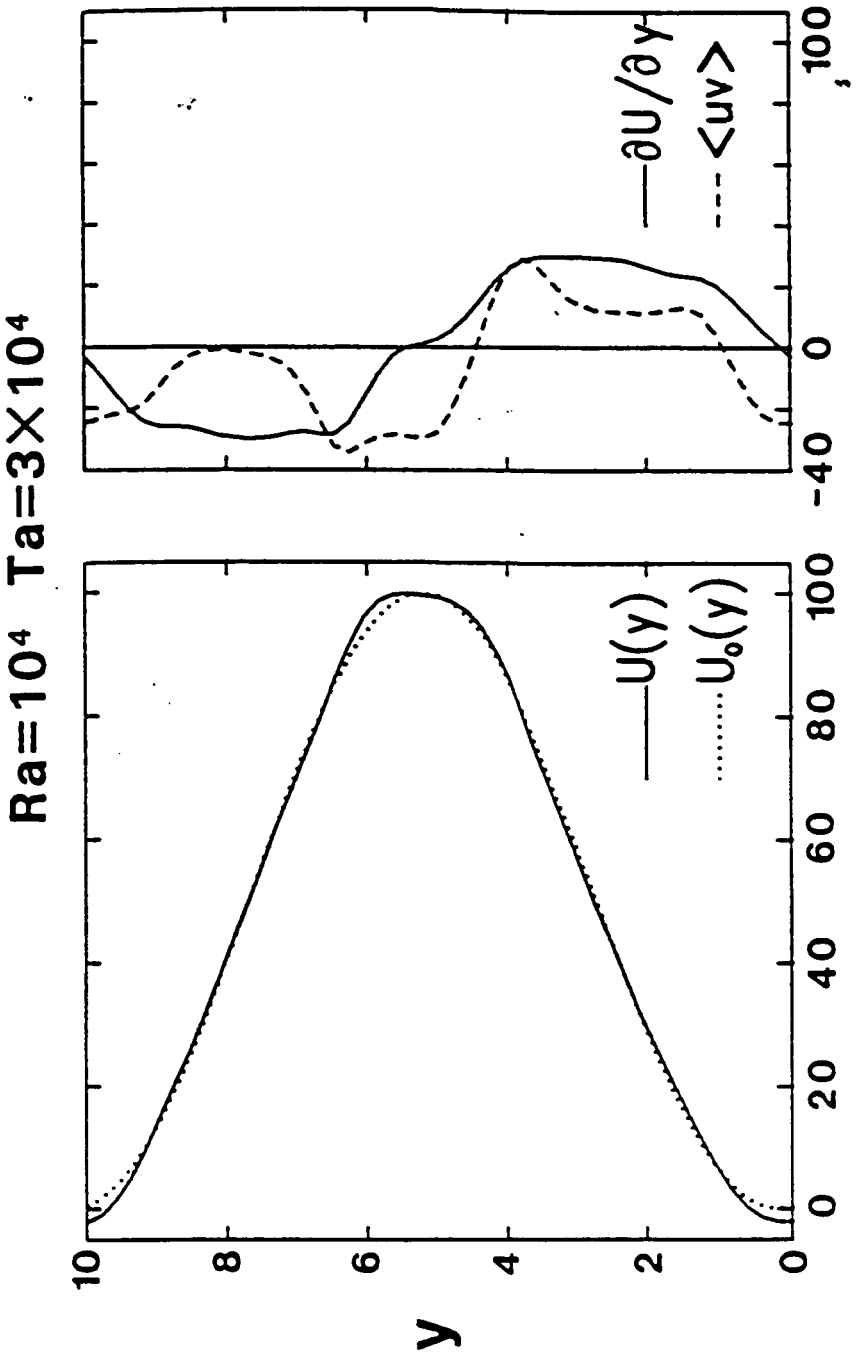

Figure 9

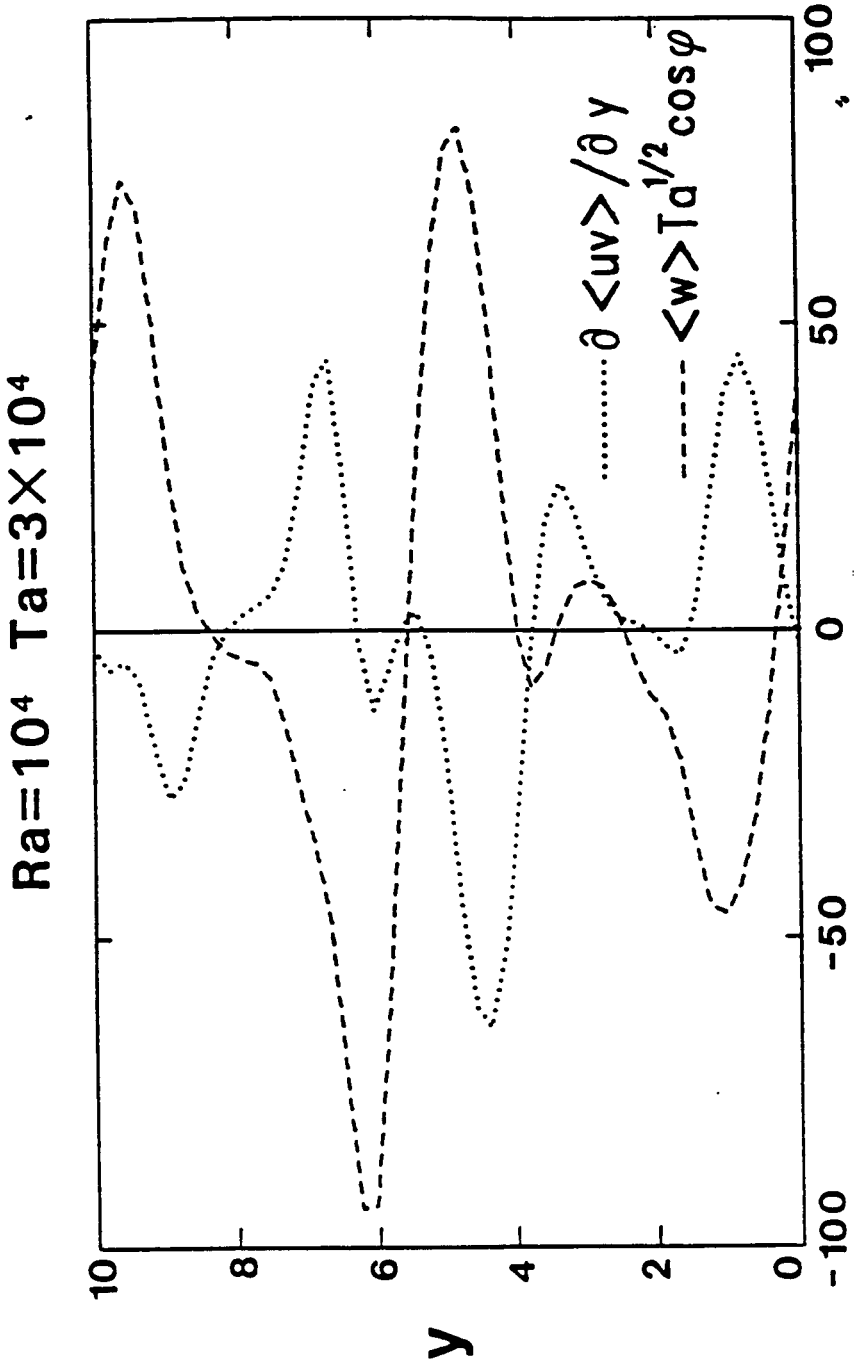

Figure 10

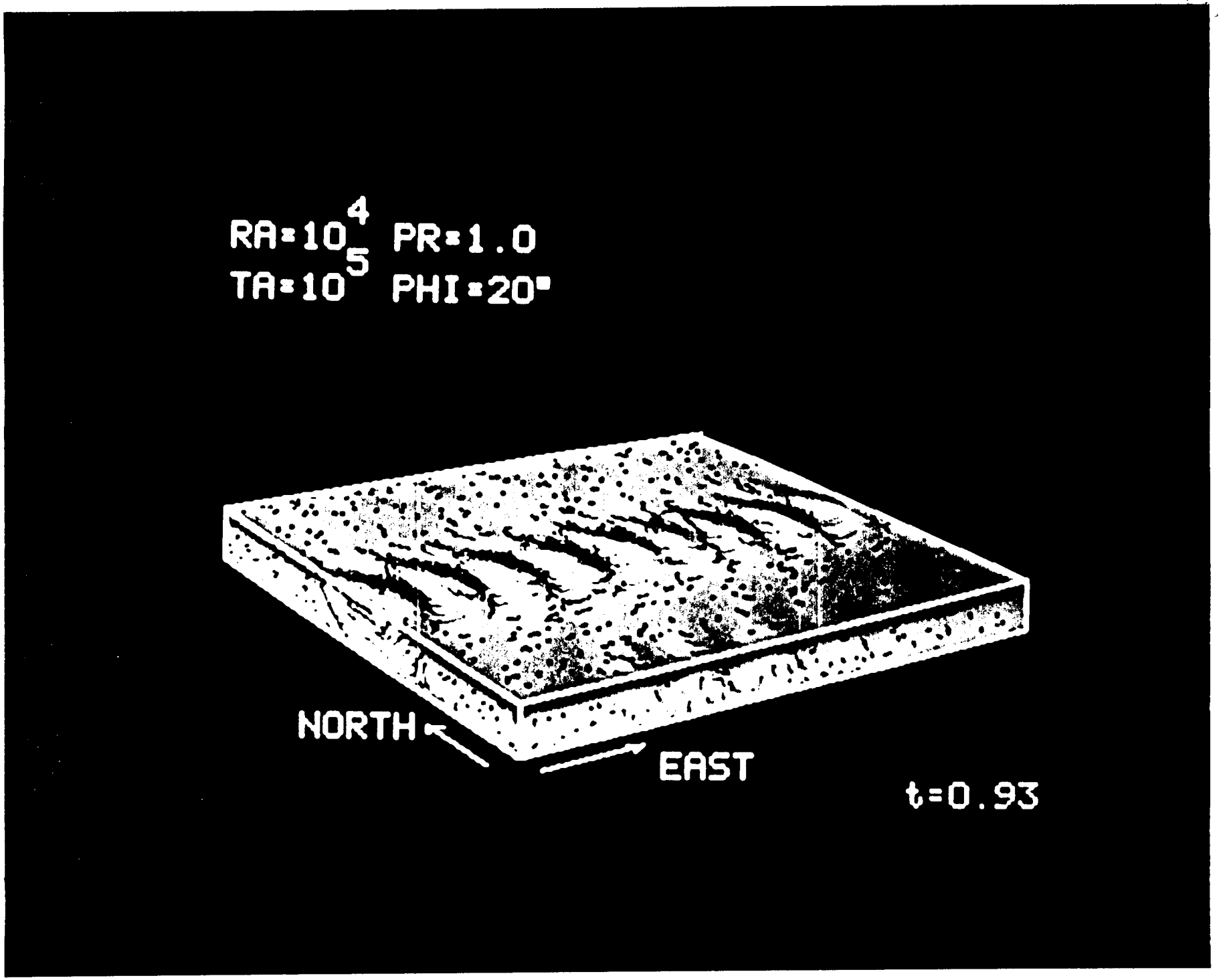
RA=10^4 PR=1.0
TA=10^5 PHI=20°
NORTH
EAST
t=0.93

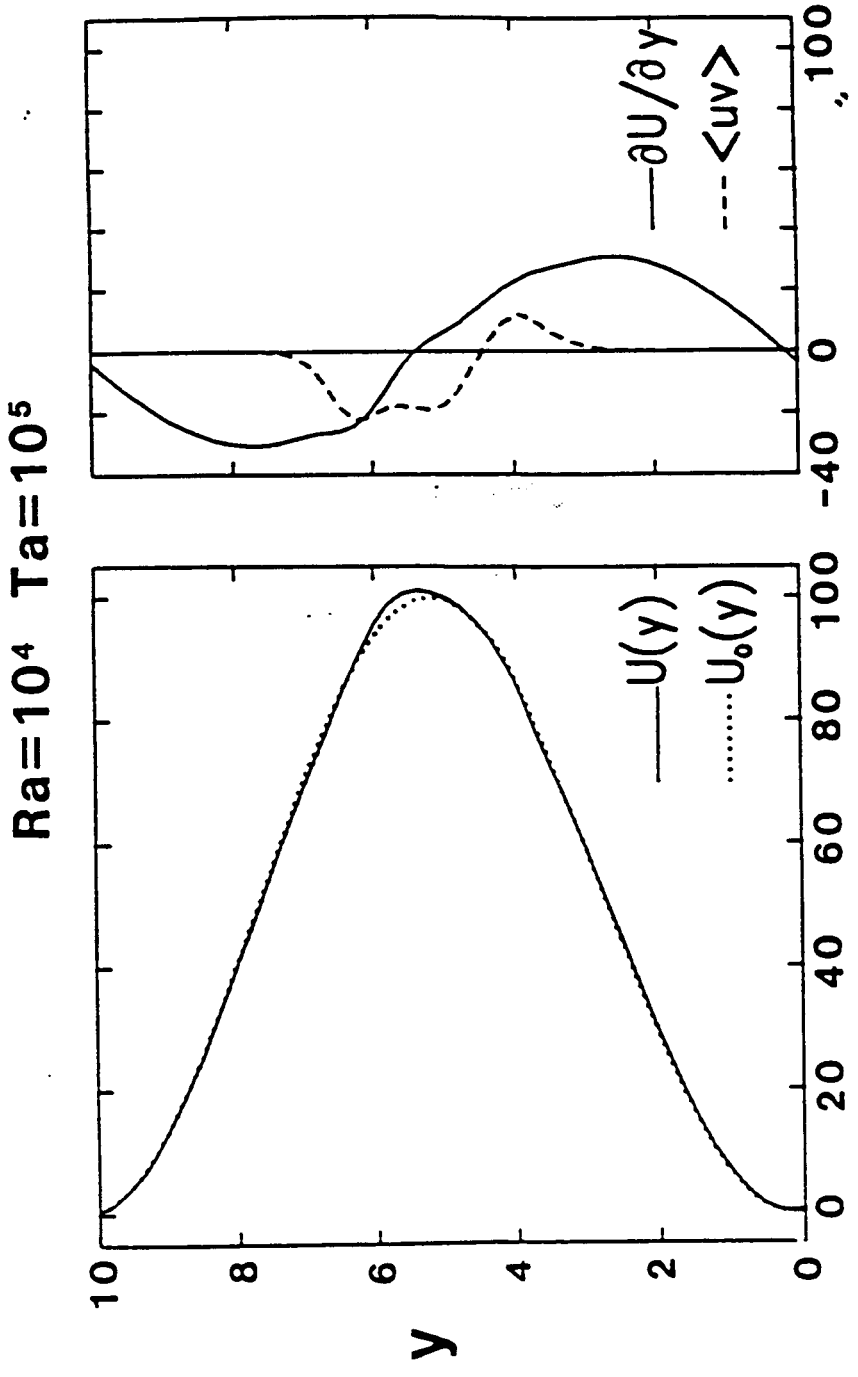

Figure 12

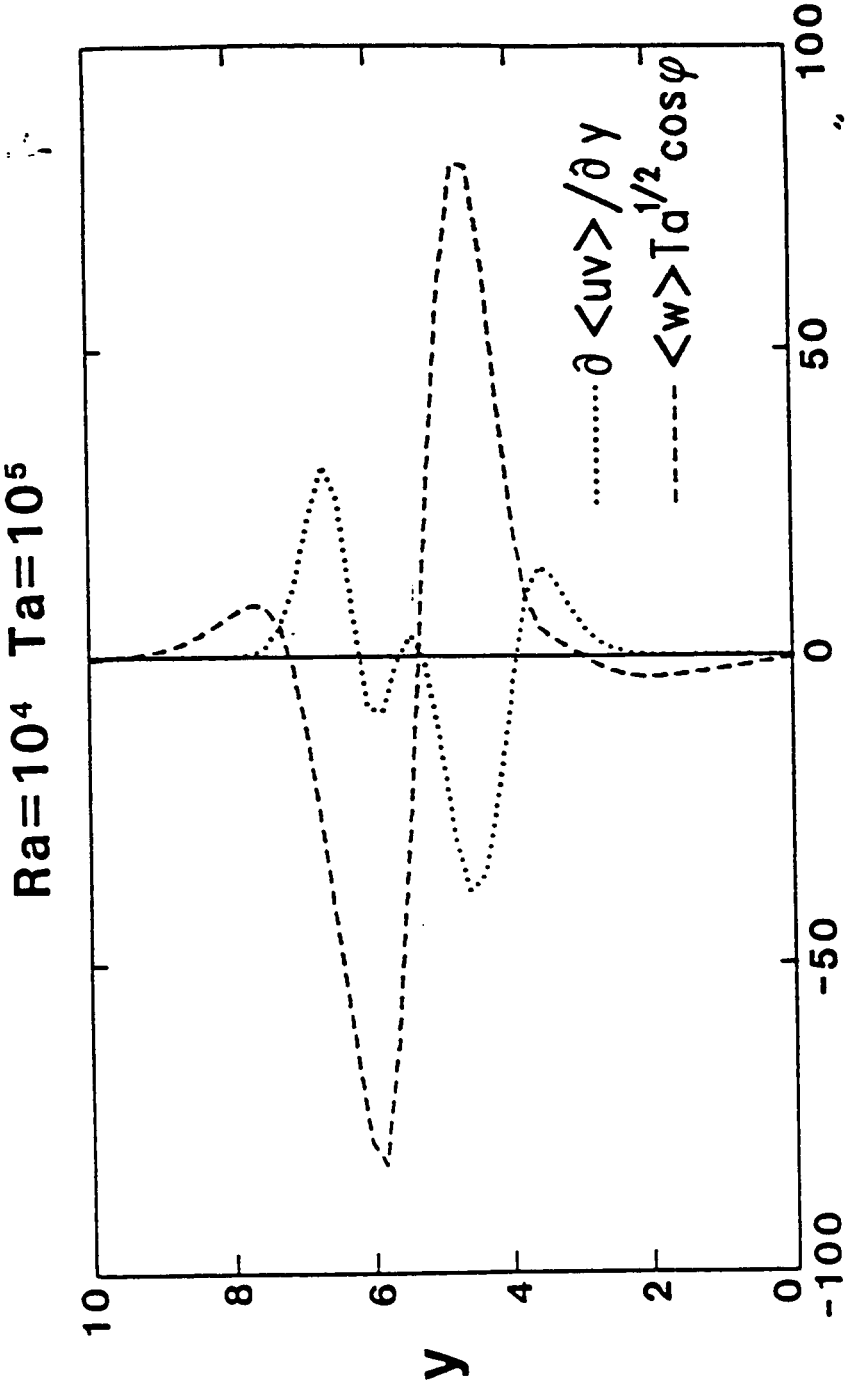

Figure 13

Figure 14